NEURON-ASTROCYTE SIGNALING IS PRESERVED IN THE AGEING BRAIN

Marta Gómez-Gonzalo[1,*], **Mario Martin-Fernandez**[2,*], **Ricardo Martínez-Murillo**[1,*], **Sara Mederos**[1], **Alicia Hernández-Vivanco**[1], **Stephanie Jamison**[2], **Ana P. Fernandez**[1], **Julia Serrano**[1], **Pilar Calero**[1], **Hunter S. Futch**[4], **Rubén Corpas**[4], **Coral Sanfeliu**[3], **Gertrudis Perea**[1,†], and **Alfonso Araque**[2,†]

[1]Instituto Cajal, CSIC. Madrid, 28002, Spain

[2]Dept. Neuroscience, University of Minnesota. Minneapolis, 55455, USA

[3]Aging and Neurodegeneration Unit, Biomedical Research Institute of Barcelona (IIBB), CSIC and IDIBAPS, 08036, Barcelona, Spain

[4]College of Medicine, University of Florida, Gainesville, FL 32610-0261, USA

Abstract

Astrocytes play crucial roles in brain homeostasis and are emerging as regulatory elements of neuronal and synaptic physiology by responding to neurotransmitters with Ca^{2+} elevations and releasing gliotransmitters that activate neuronal receptors. Ageing involves neuronal and astrocytic alterations, being considered risk factor for neurodegenerative diseases. Most evidence of the astrocyte-neuron signaling is derived from studies with young animals; however, the features of astrocyte-neuron signaling in adult and aging brain remain largely unknown. We have investigated the existence and properties of astrocyte-neuron signaling in physiologically and pathologically ageing mouse hippocampal and cortical slices at different lifetime points (0.5 to 20 month-old animals). We found that astrocytes preserved their ability to express spontaneous and neurotransmitter-dependent intracellular Ca^{2+} signals from juvenile to ageing brains. Likewise, resting levels of gliotransmission, assessed by neuronal NMDAR activation by glutamate released from astrocytes, were largely preserved with similar properties in all tested age-groups, but DHPG-induced gliotransmission was reduced in aged mice. In contrast, gliotransmission was enhanced in the APP/PS1 mouse model of Alzheimer's disease, indicating a dysregulation of astrocyte-neuron signaling in pathological conditions. Disruption of the astrocytic IP_3R2 mediated-signaling, which is required for neurotransmitter-induced astrocyte Ca^{2+} signals and gliotransmission, boosted the progression of amyloid plaque deposits and synaptic plasticity impairments in APP/PS1 mice at early stages of the disease. Therefore, astrocyte-neuron interaction is a fundamental signaling, largely conserved in the adult and ageing brain of healthy

[†]Correspondence should be addressed to: Dr. Alfonso Araque, Dept. Neuroscience, University of Minnesota, 2101 6th Street SE, Minneapolis, MN 55455. USA, Tel: 612-624-0901, araque@umn.edu, Dr. Gertrudis Perea, Instituto Cajal, CSIC, Avda. Doctor Arce, 37, Madrid, 28002. SPAIN, Tel: (+34) 915 854 710, gperea@cajal.csic.es.
[*]These authors contributed equally to this work.
Marta Gomez-Gonzalo is currently at the Neuroscience Institute (IN) of CNR (Padova, Italy).

animals, but it is altered in Alzheimer's disease, suggesting that dysfunctions of astrocyte Ca^{2+} physiology may contribute to this neurodegenerative disease.

Keywords

Astrocytes; brain ageing; gliotransmission; neuron-glia signaling; synaptic plasticity

INTRODUCTION

Ageing entails many morphological and physiological changes of brain structure and function, which is considered to be a risk factor for many neurodegenerative disorders, such as Alzheimer's disease (AD) and Parkinson's disease, by a wide number of means, from the activation/inactivation of particular genes to environmental alteration of biochemical pathways (Maynard et al. 2015). Indeed, a great effort has been made to understand the abnormalities of neuronal and synaptic activities occurring in neurodegenerative diseases associated with aging (Hung et al. 2010), and most of the studies have focused on the analysis of the morphological and molecular changes occurring in neurons and glial cells (Lynch et al. 2010; Riddle 2007).

Astrocytes, a glial cell type, have emerged in the last years as important cells in brain function. In addition to the key roles played in brain homeostasis by controlling extracellular levels of ions and neurotransmitters, astrocytes also actively and dynamically interact with neurons, responding to neurotransmitters and regulating neuronal and synaptic function by releasing gliotransmitters (Araque et al. 2014; Eroglu and Barres 2010; Perea et al. 2014). On the other hand, astrocytic physiological dysfunctions, including alterations of the astrocyte calcium (Ca^{2+}) signal (Delekate et al. 2014; Kuchibhotla et al. 2009; Takano et al. 2007), have been related with the pathology of particular neurodegenerative diseases (Rudy et al. 2015; Tong et al. 2014; Yates 2015). Most of the current knowledge of the astrocyte-influence on neuronal and synaptic function has been derived from young animal studies (Agulhon et al. 2008; Araque et al. 2014), but the functional properties of the astrocyte-neuron signaling in ageing brain, in either healthy or pathological conditions, remain largely unknown (Grosche et al. 2013; Navarrete et al. 2012b; Peters et al. 2009; Sun et al. 2013; Tang et al. 2015).

Here, we investigated the fundamental features of astrocyte-neuron signaling i.e., astrocyte responsiveness to neurotransmitters and synaptic activity, and astrocyte ability to release glutamate and impact neuronal activity, at different stages of adult life and ageing. Our results show that the intrinsic and neurotransmitter-evoked Ca^{2+} signaling in astrocytes is downregulated but largely preserved in brain slices from adult and aged mice. Likewise, neuronal NMDAR-dependent currents evoked by astrocyte glutamate release were similarly present in adult and aged animals. However, in APP/PS1 AD mouse model the astrocytic gliotransmission was significantly increased. The downregulation of IP_3R2-mediated Ca^{2+} signaling in astrocytes stimulated an accelerated progression of amyloid plaques and synaptic plasticity deficits in APP/PS1 AD mouse model. Taken together, present results show that neuron-astrocyte communication is a fundamental signaling pathway in the brain

present in the adult life as well as in ageing, and that dysfunctions of the astrocyte Ca^{2+} signal contribute to the progression of Alzheimer's disease.

MATERIALS AND METHODS

Animals

All the procedures for handling and sacrificing animals followed the European Commission guidelines for the welfare of experimental animals (2010/63/EU). All experimental and animal care procedures complied with US National Institutes of Health guidelines and were approved by the Animal Welfare Committee of the Cajal Institute and by the Institutional Animal Ethics Committee of CSIC (R.D. 53/2013). A special effort was made to reduce the number of animals used in the study. Mice of both genders were used. Animals were housed under 12/12-h light/dark cycle and up to five animals per cage. No relevant behavioral features were observed in aged mice, i.e., sedentary behavior.

Brain slices and electrophysiology

Hippocampal and somatosensory cortical slices were obtained from C57BL/6 wild type mice and inositol 1,4,5-triphosphate-type 2 receptor (IP_3R2) knockout ($IP_3R2^{-/-}$) mice (Li et al. 2005) at different ages: 0.5, 5, 12, 20 months. Senescence-accelerated prone mouse 8 (SAMP8) and senescence-accelerated-resistant mouse 1 (SAMR1) were analyzed at 6 months. APPswe/PS1 E9 (Jankowsky et al. 2001), termed APP/PS1 in this study, were analyzed at 12 months. Offspring of crossbred APP/PS1 and IP_3R2 transgenic mice were analyzed at 6 and 2.5–3 months. Mice were anaesthetized, decapitated and brains were rapidly removed and placed in ice-cold artificial cerebrospinal fluid (ACSF). Slices (350–400 μm) from juvenile mice were incubated during >1 h at room temperature (22–24° C) in ACSF containing (in mM): NaCl 124, KCl 2.69, KH_2PO_4 1.25, $MgSO_4$ 2, $NaHCO_3$ 26, $CaCl_2$ 2, Sodium Ascorbate 0.4, and Glucose 10, and was gassed with 95% O_2 / 5% CO_2 (pH = 7.3–7.4). To reduce swelling and damage in superficial layers of the slices from adult and ageing mice, slices were obtained with either modified ACSF containing (in mM): NaCl 75, KCl 2.69, KH_2PO_4 1.25, $MgSO_4$ 2, $NaHCO_3$ 26, $CaCl_2$ 2, Glucose 10, Sucrose 100, Sodium Ascorbate 1, and Sodium pyruvate 3; and modified N-methyl-D-glucamine (NMDG)-ACSF, as substitute for sodium ions in a wide range of adult ages and applications (Ting et al. 2014), containing (in mM): NMDG 93, KCl 2.5, NaH_2PO_4 1.2, $NaHCO_3$ 30, HEPES 20, $MgSO_4$ 10, $CaCl_2$ 0.5, Glucose 25, Sodium Ascorbate 5, Thiourea 2, Sodium pyruvate 3, gassed with 95% O_2 / 5% CO_2 (pH = 7.3–7.4). Slices obtained with (NMDG)-ACSF were incubated during 10 min at 32°C before being transferred at regular ACSF (room temperature) for 1 h incubation previous to the recordings. Slices were then transferred to an immersion recording chamber and superfused with gassed regular ACSF. Cells were visualized under an Olympus BX50WI microscope. Electrophysiological patch-clamp recordings from CA1 pyramidal and layer 2–3 cortical neurons were made using patch electrodes (3–6 MΩ) filled with the internal solution (in mM): K-Gluconate 135, KCl 10, HEPES 10, $MgCl_2$ 1, ATP-Na_2 2 (pH = 7.3, with KOH), and the membrane potential was held at −70 mV to record EPSCs and slow inward currents (SICs). For SICs recordings ACSF was adjusted with $CaCl_2$ 4mM, glycine 10 μM, zero magnesium and TTX 1 μM. Signals were digitized at 10.0 kHz. Trains of stimuli to SC afferents were delivered at 30 Hz

during 5 s and astrocyte responsiveness to SC synaptic activity was isolated by picrotoxin (50 μM) and CGP55845 (5μM), GABAa and GABAb receptors antagonists, respectively (Fig. 3A). Experiments were performed at room temperature (22–24 °C) unless indicated. For extracellular recordings, the stimulation and recording electrodes (2–4 MΩ; filled with NaCl 3 mM) were placed on the *stratum radiatum*. Extracellular excitatory postsynaptic field potentials (fEPSPs) were bandpass filtered between 0.3 Hz and 1.0 kHz, and digitized at 10.0 kHz. Ten min baseline responses at 0.1 Hz. were recorded before LTP-induction protocol (100 Hz trains delivered 4 times at 0.05 Hz). Extracellular recordings were performed at 32 °C. The pCLAMP 10 software (Molecular Devices) was used for stimulus generation, data display, acquisition, storage and analysis.

Ca^{2+} imaging

Animals were injected intraperitoneally with sulforhodamine 101 (SR101; 100 mg/kg) and left in the cage with food and water for 1–2 h before removing the brain (Perez-Alvarez et al. 2014). Ca^{2+} levels in astrocytes specifically loaded with SR101 (Fig. 1B; Fig. 2A), were monitored by fluorescence microscopy using the Ca^{2+} indicator Fluo-4-AM (Nimmerjahn et al. 2004; Perez-Alvarez et al. 2014). Cells were illuminated during 100–500 ms with a xenon lamp at 490 nm using a monochromator Polychrome V (Till Photonics). Images were acquired every 0.5–1 s and analyzed by the IPLab software. Astrocytic Ca^{2+} signals were recorded from the cell body and Ca^{2+} levels were estimated as changes in the fluorescence signal over the baseline (F/F0). The Ca^{2+} oscillation frequency was obtained from the number of Ca^{2+} spikes occurring in 6 to 15 astrocytes in the field of view during 10 min of recording. Astrocyte Ca^{2+} signals were quantified as the number of Ca^{2+} elevations in 5 s bins, termed Ca^{2+} spike probability, and mean values were obtained by averaging different experiments (Gomez-Gonzalo et al. 2015; Navarrete et al. 2012a). Ca^{2+} spike probability changes over mean baseline were evaluated 15 s before the stimulus and maximum Ca^{2+} spike probability recorded 15 s after stimulus (Fig. 2B). Local application of ATP (4 mM), DHPG (1 mM), TFLLR (1 mM) and ACh (2 mM) were delivered by 5 s duration pressure pulses through a micropipette in the presence of TTX (1 μM).

Immunohistochemistry

Distribution and density of amyloid plaques were investigated by histochemistry in offspring APP/PS1-IP$_3$R2 mice (n = 8 for all tested groups). Experiments were performed at 2–3 months and 6 months-old female mice. Mice were processed according to standard procedures described previously (Muneton-Gomez et al. 2012). Briefly, after brain fixation with 4% (w/v) paraformaldehyde in 0.1 M PB, tissue was cryopreserved in 30% sucrose in 0.1M PB and cut into blocks. Coronal slices (30 μm) were obtained with the aid of a Leica cryostat and selected sections (10 sections per case) obtained between Bregma levels: AP −1.3 mm and −2.20 mm, according to Paxinos and Franklin (Paxinos 2012), were processed by the Thioflavin S staining procedure (Bussiere et al. 2004). Images were acquired at 10x magnification and the number of Thioflavin S-positive plaques was measured by automatic outlining of their perimeter with the appropriate plugin of ImageJ software (http://rsbweb.nih.gov/ij/). To prevent bias all the analysis was done blinded to the animal information. No amyloid plaques were found in APP/PS1$^{−/−}$-IP$_3$R2$^{+/+}$ and APP/PS1$^{−/−}$-

IP$_3$R2$^{-/-}$ mice (0 plaques), indicating that the absence of the astrocyte IP$_3$R2-mediated signaling does not induce Aβ pathology.

Alternatively, protein analysis of IP$_3$R2 levels in either APP/PS1$^{+/+}$-IP$_3$R2$^{-/-}$ and APP/PS1$^{+/+}$-IP$_3$R2$^{+/+}$ mice (4 month-old) was performed by immunohistochemistry. Selected free-floating paraformaldehyde fixed sections obtained similar as for Thioflovin S procedure, were processed by the avidin-biotin peroxidase complex (ABC) technique. Endogenous IP$_3$R2 protein was visualized with anti-IP$_3$R2 (1:20, AB3000; Millipore) antibody. No IP$_3$R2 protein labelling was observed in APP/PS1$^{-/-}$-IP$_3$R2$^{-/-}$ mice (Fig. 4E).

Genotyping

Offspring from APP/PS1-IP$_3$R2 intercrosses were genotyped by PCR analysis as described by (Li et al. 2005) from DNA extracted from either tail clip or paraformaldehyde fixed brain sections of the same animals processed for histochemistry (Fig. 4E), showing specific bands ~200bp and ~400bp corresponding to IP$_3$R2 wildtype gene and IP$_3$R2 transgene, respectively.

Drugs

(S)-(+)-α-Amino-4-carboxy-2-methylbenzeneacetic acid (LY-367385), 2-Methyl-6-(phenylethynyl)pyridine hydrochloride (MPEP), D-(−)-2-Amino-5-phosphonopentanoic acid (D-AP5), 3,5-dihydroxyphenylglycine (RS-3,5-DHPG), 8,8'-[Carbonylbis[imino-3,1-phenylenecarbonylimino(4-methyl-3,1-phenylene)carbonylimino]]bis-1,3,5-naphthalenetrisulfonic acid hexasodium salt (suramin), and Protease-Activated Receptors TFLLR-NH2 were purchased from Tocris. The Ca^{2+} indicator Fluo-4-AM was purchased from Life Technologies Ltd. Picrotoxin, atropine, ATP and other drugs were purchased from Sigma-Aldrich.

Statistical Analysis

Data are expressed as mean ± standard error of the mean (SEM). N 5 mice per age-group and condition were analyzed unless indicated. Normality test was performed before applying statistical comparisons, which were made using non parametric Rank-sum test and parametric Student's t tests as deemed appropriate. Two-tailed, unpaired or paired test was used for comparisons unless indicated. ANOVA followed by post hoc test was applied for multiple comparisons. Statistical differences were established with P < 0.05 (*), P < 0.01 (**), and P < 0.001 (***, #).

RESULTS

Astrocyte excitability based on intracellular Ca^{2+} variations can occur spontaneously or can be evoked by neurotransmitters released during neuronal activity (Nett et al. 2002; Perea and Araque 2005). To investigate the ability of astrocytes to display spontaneous Ca^{2+} activity during the mice lifespan, we analyzed the spontaneous Ca^{2+} excitability of hippocampal and cortical astrocytes in brain slices from juvenile (P12–17, referred as 0.5 month-old), adult (5, 12 month-old) and aged mice (20 month-old; Fig. 1A). Astrocytes were identified by sulforhodamine 101 staining and Ca^{2+} levels monitored using the Ca^{2+} indicator fluo-4-AM

(Fig. 1B). We first evaluated the intrinsic astrocyte Ca^{2+} excitability independent of action potential-mediated neuronal activity (i.e., recorded in the presence of 1 μM tetrodotoxin, TTX) at different ages (Fig. 1B–D), quantifying the proportion of "active astrocytes" (i.e., those that showed at least one spontaneous Ca^{2+} elevation during the 10 min recording) and the number of Ca^{2+} elevations (Fig. 1C, D). At all ages analyzed, both hippocampal and cortical astrocytes displayed spontaneous activity, but, in both areas, slices from 0.5 month-old mice showed a higher number of active astrocytes than adult and aged animals (Fig. 1C, D). Remarkably, the frequency of Ca^{2+} elevations per active cell was not altered in all tested groups (Fig. 1C, D). These results indicate that while the ability of active astrocytes to generate Ca^{2+} elevations is preserved, the number of astrocytes showing spontaneous Ca^{2+} signaling decreases after maturation and then remain stable during maturity and aging.

A remarkable feature of neuron-astrocyte signaling is the ability of astrocytes to detect neuronal activity. Studies from juvenile rodents have shown that astrocytes express a plethora of membrane receptors that upon activation by different neurotransmitters including glutamate, GABA, ATP, norepinephrine, acetylcholine or endocannabinoids (Araque et al. 2014), elicit intracellular Ca^{2+} elevations. Some reports have found different astrocyte responsiveness to neurotransmitters in early adult mice (2–3 month-old) (Otsu et al. 2015; Sun et al. 2013), although the potentially aged-dependent regulation of transmitter receptor function remains controversial (see Discussion). We then assessed the Ca^{2+} responsiveness of astrocytes to different agonists during ageing (Fig. 2A–C). In the presence of TTX (1 μM), to avoid indirect effects by neuronal co-activation, we first analyzed purinergic and cholinergic signaling by locally applying ATP (4 mM) and ACh (2 mM), respectively. The application of these transmitters induced similar responses at all ages tested (Fig. 2A–C). Astrocytic Ca^{2+} responses were blocked in 5 month-old slices by the non-selective P2 purinergic receptor antagonist suramin (50 μM; from 0.97 ± 0.06 to 0.32 ± 0.02 Ca^{2+} spike probability; P < 0.001, paired t-test; n = 68 astrocytes; n = 6 slices), and the broad muscarinic antagonist receptor atropine (50 μM; from 0.37 ± 0.02 to 0.04 ± 0.02; Ca^{2+} spike probability; P < 0.001; paired t-test; n = 71 astrocytes; n = 8 slices); indicating the selective stimulation of purinergic and muscarinic receptors by these agonists, respectively. We then tested the astrocytic sensitivity to the activation of the Protease activated receptor-1 (PAR1), which has prominent expression in astrocytes and stimulates Ca^{2+} signaling in astrocytes (Gomez-Gonzalo et al. 2010; Shigetomi et al. 2008), by local application of the agonist TFLLR (1 mM). Although most astrocytes in adult and aged mice responded to this agonist, the proportion of responding astrocytes was significantly decreased at 5, 12 and 20 months of age compared to juvenile astrocytes (P = 0.013, P 0.001, and P = 0.001; respectively; ANOVA followed by Student-Newman-Keuls test) (Fig. 2B, C). These results indicate that although the astrocytic responsiveness to certain agonists, such as TFLLR, can be aged-dependently regulated, the astrocyte Ca^{2+} signal may be stimulated by different transmitters at all ages.

Because glutamate is known to trigger astrocyte Ca^{2+} elevations through activation of group I metabotropic GluRs (Bradley and Challiss 2012), we analyzed glutamatergic signaling on astrocyte Ca^{2+} excitability during ageing by local application of the specific agonist of group I mGluRs DHPG (1 mM). Figures 2D and 2E show that both hippocampal and cortical astrocytes responded to DHPG at all ages tested with similar temporal profiles of the Ca^{2+}

responses (Fig. 2D). Notably, although more than 50% of cortical and ~ 50 % of hippocampal astrocytes were stimulated by DHPG, the proportion of responding astrocytes in both brain areas was reduced in adult and aged compared to juvenile mice ($P < 0.05$; ANOVA followed by Student-Newman-Keuls test; Figure 2E). To confirm that DHPG-induced responses in adults were mediated by activation of group I mGluRs and G protein-mediated Ca^{2+} mobilization, we tested in slices from 5 month-old mice the sensitivity of the responses to the specific antagonists of group I mGluRs MPEP (50 μM; $mGluR_5$ antagonist) and LY367385 (100 μM; $mGluR_1$ antagonist), in wild type and $IP_3R2^{-/-}$ mice (Fig. 2F). DHPG-evoked responses were significantly reduced in the presence of these antagonists, and, in agreement with previous data (Di Castro et al. 2011; Navarrete et al. 2012a; Petravicz et al. 2008), no astrocyte somatic Ca^{2+} responses were observed after DHPG stimulation in $IP_3R2^{-/-}$ mice (Fig. 2F). While a recent study has reported a developmental downregulation of the relative expression of mGluR5 *vs* mGluR3 (Sun et al. 2013), these results indicate that the expression of group I mGluRs remained sufficient to support the mGluR-mediated astrocyte Ca^{2+} signaling in adult and aged mice (Tang et al. 2015).

We then analyzed whether the mGluR-mediated astrocyte Ca^{2+} signaling could be induced by glutamate released during synaptic activity by stimulating Schaffer collaterals (SC), the main glutamatergic input to the hippocampal CA1 region, that are known to evoke mGluR-dependent astrocyte Ca^{2+} elevations in juvenile mice (Pasti et al. 1997; Perea and Araque 2005). The proportion of responding astrocytes to SC stimulation was not significantly different among all tested groups (Fig. 3A, B). Astrocytes from $IP_3R2^{-/-}$ mice lacked SC-evoked somatic Ca^{2+} signals, confirming that SC-evoked responses were mediated by synaptically-released glutamate, activating G protein-coupled receptors in all ages tested (Fig. 3B). Thus, present results show that the observed astrocytic ability to sense glutamatergic synaptic activity in juvenile mice persists in the adults as well as in aged animals.

Astrocyte Ca^{2+} increases are known to stimulate the release of different neuroactive substances, called gliotransmitters, such as glutamate, ATP, or D-serine, that can impact neuronal and synaptic activity and plasticity (Araque et al. 2014). In juvenile mice, glutamate released by astrocytes induces slow inward currents (SICs) in neurons through activation of postsynaptic NMDA receptors (Fellin et al. 2004; Kozlov et al. 2006; Perea and Araque 2005; Shigetomi et al. 2008). Then, we investigated whether the astrocyte ability to release glutamate was still present after maturation by recording neuronal whole-cell currents. Spontaneous SICs, which were sensitive to the NMDA receptor antagonist AP5 (50 μM; Fig. 3C), were found in neurons recorded from both hippocampal CA1 region and cortex in all tested groups, and no significant differences were observed in the spontaneous frequency of these currents at different ages ($P > 0.05$; ANOVA followed by Student-Newman-Keuls test; Figure 3C, F). To test the causal relationship between astrocyte Ca^{2+} activity and SICs, we stimulated astrocyte Ca^{2+} signals by local application of DHPG (1 mM; Fig. 2D), in wildtype and $IP_3R2^{-/-}$ mice (Fig. 3E, F). Both hippocampal and cortical neurons from wildtype mice increased the SIC frequency in juvenile (0.5 month old; $P = 0.04$; paired t-test) and adult mice (5–12 months-old; $P = 0.004$ and $P = 0.04$; paired t-test; respectively. Fig. 3E, F), whereas no SIC frequency changes occurred after DHPG application in either hippocampal or cortical neurons from $IP_3R2^{-/-}$ mice ($P > 0.05$; paired

t-test; Fig. 3F), confirming that IP$_3$R2-mediated astrocyte Ca^{2+} signal was necessary to induce glutamate-evoked SICs. These results indicate that the Ca^{2+}-dependent glutamate release and the subsequent NMDA receptor activation in neurons are conserved phenomena in adulthood. Notably however, in aged (20 month-old) mice, we failed to detect DHPG-evoked increases of SICs in either in hippocampal or cortical neurons (1.04 ± 0.15 *vs* 1.18 ± 0.36 SICs/ min in control and after DHPG; n = 16 hippocampal neurons; P = 0.74; Wilcoxon signed rank test; 1.19 ± 0.21 *vs* 1.55 ± 0.44 SICs/ min in control and after DHPG; n = 9 cortical neurons; P = 0.33; paired t-test; Fig. 3F). Simultaneous astrocyte Ca^{2+} signals and neuronal SICs were recorded before and after DHPG stimulation in a subset of experiments confirming the astrocytic Ca^{2+} responsiveness and the absence of evoked gliotransmission by DHPG in aged mice (1.39 ± 0.16 *vs* 2 ± 0.85 SICs/ min in control and after DHPG; n = 6 hippocampal neurons; P = 1; Wilcoxon signed rank test). Since DHPG was able to elevate astrocytic Ca^{2+} (Fig. 2E), but failed to boost glutamatergic SIC frequency over the resting tone in 20 month-old mice, which were indicative of functional neuronal NMDARs, these results might suggest deficiencies in the intracellular pathways downstream of the astrocyte Ca^{2+} signal linked to the evoked gliotransmission in aged brain.

Interestingly, in resting conditions neurons from juvenile and adult wildtype and IP$_3$R2$^{-/-}$ mice displayed similar SIC frequencies (Fig. 3C, F), whereas somatic Ca^{2+} elevations were scarce in IP$_3$R2$^{-/-}$ mice (Fig. 3D) (Chen et al. 2012; Navarrete et al. 2012a; Petravicz et al. 2008). However, Ca^{2+} fluctuations have been reported in astrocyte processes in brain slices and *in vivo* IP$_3$R2$^{-/-}$ mice (Srinivasan et al. 2015). Although present data do not discard that resting levels of astrocyte glutamate release might occur by independent IP$_3$R2-mediated pathways or by Ca^{2+}-dependent mechanisms restricted to astrocytic processes, these results do show that the neurotransmitter-induced glutamate released from astrocytes requires the activation of global, including soma, IP$_3$R2-mediated Ca^{2+} signaling.

In order to further assess whether gliotransmission was affected by aging, we evaluated the astrocyte-neuron signaling in a mouse model showing a phenotype of accelerated ageing, the spontaneous senescence accelerated SAMP8 mice (Takeda 1999), which show age-associated behavioral impairments including learning and memory difficulties (Lopez-Ramos et al. 2012; Tomobe and Nomura 2009). Recordings from 6 month-old mice showed that the SIC frequency recorded from hippocampal and cortical neurons were not significantly different in SAMP8 mice and the corresponding control mice SAMPR1 (resistant strain to early senescence; Fig. 3G). These results indicate that gliotransmission mechanisms were preserved in the spontaneous accelerated ageing mouse model, which agrees with results observed in wildtype mice that physiologically reached ageing (0.77 ± 0.17 SICs/min and 1.04 ± 0.16 SICs/min in SAMP8 (6 months) and wildtype mice (20 months), respectively; P = 0.714; unpaired t- test; Fig. 3C, G). Taken together, these results suggest that gliotransmission, originally found in young animals, is a conserved phenomenon that persists in adulthood and senescence.

Ageing is a key factor in the appearance and progress of numerous neurodegenerative diseases. Indeed, AD is an age-related neurodegenerative condition characterized by progressive decline in cognitive function and widespread depositions of amyloid plaques and neurofibrillary tau pathology in the brain (Braak and Braak 1991). Recent studies have

reported an enhanced Ca^{2+} excitability in mouse cortical astrocytes near amyloid β (Aβ) plaques (Kuchibhotla et al. 2009), and increased astrocyte Ca^{2+} elevations and neuronal SICs in juvenile hippocampal slices acutely treated with Aβ oligomers (Pirttimaki et al. 2013; Talantova et al. 2013). We therefore investigated the potential alterations of the properties of astrocyte-neuron signaling in AD, using the APP/PS1 transgenic mouse model. Recordings from hippocampal and cortical neurons from 12 month-old APP/PS1 mice, which showed advanced AD symptoms (Bilkei-Gorzo 2014), exhibited an increased SIC frequency in resting conditions compared with control matched-age mice (Fig. 4B) (Pirttimaki et al. 2013); indicative of an increased tone of glutamatergic gliotransmission in APP/PS1 mice. Furthermore, as observed in wildtype mice (see Fig. 3F), astrocyte stimulation by local application of DHPG evoked higher rates of SICs in these mice (Fig. 4A, B), indicating that neurotransmitter-evoked gliotransmission was also present in APP/PS1 transgenic mice and the boosted astrocyte-neuron signaling occurring in AD pathology was not saturated.

Amyloid deposition is considered a hallmark of AD (Palop and Mucke 2010). The APP/PS1 mouse model begins to develop plaques at about 3–4 months-old and the number of plaques increases with age (Bilkei-Gorzo 2014). Reliably, cognitive impairments and synaptic plasticity deficits are found from 5–7 months (Schaeffer et al. 2011). Thus, considering that astrocyte Ca^{2+} signaling and gliotransmission are enhanced in APP/PS1 mice, we then investigated the influence of the astrocytic Ca^{2+} signaling on Aβ pathology *in vivo*. We crossbred APP/PS1 and $IP_3R2^{+/-}$ transgenic lines to generate APP/PS1$^{+/+}$-$IP_3R2^{-/-}$ mice that express APP/PS1 genes and have impaired the IP_3R2-mediated Ca^{2+} signal. At 6 months of age, the cortex and hippocampus of these mice showed a remarkable enhanced deposition of thioflavin S-positive amyloid plaques when compared to APP/PS1$^{+/+}$-$IP_3R2^{+/+}$ control littermates (n = 8; Fig. 4C, D). In addition, the amyloid deposits can be observed as early as 2–3 months-old in APP/PS1$^{+/+}$-$IP_3R2^{-/-}$ mice (n = 8; Fig. 4C, D). However, no amyloid plaques were found in APP/PS1$^{-/-}$-$IP_3R2^{+/+}$ or APP/PS1$^{-/-}$-$IP_3R2^{-/-}$ mice, indicating that the absence of the astrocyte IP_3R2-mediated signaling does not induce Aβ pathology. Our crossbred model was also processed by immunohistochemistry to study the distribution of endogenous IP_3R2 protein. As expected, in APP/PS1$^{+/+}$ $IP_3R2^{+/+}$ mice IP_3R2 protein was located in astrocyte-like cells, while no labelling was found in APP/PS1$^{+/+}$ $IP_3R2^{-/-}$ mice (Fig. 4E), confirming the targeted deletion of IP_3R2 protein in APP/PS1$^{+/+}$-$IP_3R2^{-/-}$ mice. To test the effects on synaptic plasticity, we then analyzed the potential impairments of hippocampal CA3-CA1 synaptic plasticity at 2–3 months of age, when the amyloid plaque deposition began to be observed in APP/PS1$^{+/+}$-$IP_3R2^{-/-}$ mice. We recorded the long-term plasticity in the field excitatory postsynaptic potentials (fEPSPs) evoked by high frequency stimulation of SC (Fig. 4F, G). While wildtype mice (APP/PS1$^{-/-}$-$IP_3R2^{+/+}$), littermates with only impaired IP_3R2-mediated signaling (APP/PS1$^{-/-}$-$IP_3R2^{-/-}$), and littermates expressing APP/PS1 with normal IP_3R2-mediated signaling (APP/PS1$^{+/+}$-$IP_3R2^{+/+}$) displayed similar LTP magnitudes (n = 12, 14 and 9, respectively; P < 0.001; P = 0.008; P < 0.001; respectively); mice expressing APP/PS1 with impaired IP_3R2-mediated signaling (APP/PS1$^{+/+}$-$IP_3R2^{-/-}$) showed a significant impairment of LTP (n = 12; P = 0.39) compared with APP/PS1$^{+/+}$-$IP_3R2^{+/+}$ littermates (n = 12 and 9, respectively; P < 0.001; Fig. 4F, G). These results, which agree with the reported absence of cognitive impairments and

synaptic plasticity deficits at this early age (Jo et al. 2014; Schaeffer et al. 2011), and the normal HFS-evoked LTP in mice with astrocyte-downregulated IP$_3$R2 signaling (n = 14; P = 0.008; cf. (Agulhon et al. 2010; Shigetomi et al. 2013)), indicate that synaptic plasticity is impaired in an AD mouse model deficient of astrocyte IP3R2-mediated Ca^{2+} signal. Therefore, present results reveal that astrocytes and their IP$_3$R2-dependent Ca^{2+} signaling play crucial roles in the AD pathology, prompting an accelerated progression of the deleterious factors, such as amyloid plaques and synaptic plasticity dysfunction.

DISCUSSION

Age is directly related to numerous neurodegenerative brain disorders, and most of them are associated with astroglial dysfunctions (Maragakis and Rothstein 2006; Verkhratsky et al. 2013). Here we studied the age-dependent changes of basic functional properties of astrocyte physiology and neuron-astrocyte signaling. We found that active astrocytes expressed similar intrinsic Ca^{2+} oscillation rates during adulthood (5, 12 month-old) and ageing (20 month-old), but the number of astrocytes showing spontaneous Ca^{2+} activity measured at the soma was relatively decreased when compared to juvenile (0.5 months-old) animals, suggesting an enhanced astrocytic intrinsic excitability at early stages of development. In contrast, the spontaneous oscillatory activity displayed by active astrocytes was similar for all the tested ages (Fig. 1C, D). Because cell viability is usually weakened in slices from adult mice, damaged astrocytes might have been quantified as non-active astrocytes. Therefore, the experimental procedures might account for the observed reduction in adult and ageing brain groups. This idea is supported by the constancy of the intrinsic activity displayed by active astrocytes. Nevertheless, our results indicate that the inherent astrocytic Ca^{2+} based cell-body excitability is largely maintained during brain lifespan.

A key feature of neuron-astrocyte signaling is the ability of astrocytes to sense neurotransmitters and synaptic activity in juvenile animals. To test the astrocytic responsiveness to neurotransmitters in the adult and ageing brain we selected paradigmatic receptor agonists that are known to elevate astrocyte Ca^{2+} in juvenile animals, namely, ATP, ACh, TFLLR and DHPG. We have found that astrocyte responsiveness to these agonists was preserved in adult and aged mice; notwithstanding a relative reduction of the glutamatergic responsiveness to group I mGluR agonist DHPG (Fig. 2E). A relative developmental down-regulation of the expression of mGluR$_5$ *vs* mGluR$_3$ has recently reported (Sun et al. 2013), suggesting that astrocyte Ca^{2+} signaling mediated by glutamatergic synaptic activity, might be confined to young rodents. Present data is in agreement with a decrease in group I mGluRs expression during adulthood. However, our results also indicate that these receptors are still sufficiently present and functional to stimulate astrocytic intracellular Ca^{2+} (Fig 2F). The fact that group I mGluRs mobilize intracellular Ca^{2+} through a G protein-mediated amplifying intracellular signaling cascade, may support, even if reduced, the astrocyte responsiveness to glutamate. Taken together, these results indicate that neuron-to-astrocyte signaling, including group I mGluR-mediated glutamatergic signaling, was present and largely maintained in juvenile, adult and aged mice. These data also agree with the reported astrocyte responsiveness to neurotransmitters in adult human brain tissue (Navarrete et al., 2012a).

Since aged astrocytes showed a reduced ability to display spontaneous somatic Ca^{2+} events, but Ca^{2+} responses were elicited when stimulated with ATP or ACh with similar percentages to juvenile/adult mice (Fig. 2), that declined excitability might indicate an intrinsic property of astrocytes in ageing. Additionally, Ca^{2+}-independent mechanisms could gain significance for the astrocytic neuromodulation in the aged brain. Because our data are based on Ca^{2+} analysis restricted to the soma of the cells, and considering the relevance that Ca^{2+} signals at the level of astrocyte local processes might have on neuronal activity (Di Castro et al. 2011; Otsu et al. 2015; Panatier et al. 2011; Srinivasan et al. 2015), then whether aged astrocytes show differences in Ca^{2+} signals at the processes needs to be explored.

Astrocytes actively modulate synaptic properties via gliotransmitter release (Eroglu and Barres 2010; Perea et al. 2014). It has been established from juvenile mice that glutamate released by astrocytes can enhance postsynaptic excitability by inducing SICs mediated via neuronal NMDAR activation by astrocytic glutamate (Araque et al. 2014). Our results show that SICs, indicative of glutamatergic-mediated astrocyte gliotransmission, were present in all age-tested groups with similar rates. Moreover, gliotransmission was also found in the accelerated senescence mouse model SAMP8 at similar rates to age-matched wildtype littermates and ageing mice, suggesting a lifelong conserved level of glutamatergic astrocyte-to-neuron signaling (Navarrete et al. 2012b). It's worthy to note that particular age-related changes can take place after 20 month-old, whether the reported neuron-astrocyte signaling might be preserved or additional changes might account in advanced stages of aging require further attention.

Recent evidence has found changes in the astrocyte network coupling features in aged mice, showing that the size and astrocytic territories overlapping in cortex and hippocampus were increased (Grosche et al. 2013), which might contribute to the decreasing functional capabilities of aged astrocytes. In addition, astrocytic larger networks were found in neocortex from AD brains (Peters et al. 2009). Not only structural changes have been reported, but astrocytic Ca^{2+} signaling has also been found to be altered in certain neurological diseases (Bosson et al. 2015; Jurado-Parras et al. 2016). Cortical astrocytes in AD exhibit higher resting levels of Ca^{2+} and generate synchronous activity in the vicinity of Aβ plaques (Kuchibhotla et al. 2009). Astrocytes exposed to exogenous Aβ show an enhanced glutamatergic gliotransmission that contributes to neuronal excitability (Pirttimaki et al. 2013; Talantova et al. 2013), and synapse loss (Talantova et al. 2013). Reactive astrocytes have shown to abnormally release GABA, which has been suggested to participate in synaptic plasticity deficits and memory impairment occurring in AD (Jo et al. 2014). Our findings show that APP/PS1 mice displayed enlarged levels of glutamatergic gliotransmission both in basal conditions and after DHPG stimulation, suggesting an exacerbated rate of astrocyte-neuron signaling in AD.

Furthermore, using APP/PS1 mice, a mouse model of AD, and $IP_3R2^{-/-}$ mice, which lacks G protein-mediated Ca^{2+}signals in astrocytes, we have found that the absence of IP_3R2-mediated astrocyte Ca^{2+} signaling accelerated the progression of Aβ plaque depositions and synaptic plasticity deficits at very early stages of the disease, which suggest a protective role of astrocyte Ca^{2+} signals in the initial phase of AD pathology. Astrocytes have been shown to be implicated in metabolite clearance and removal of potentially neurotoxic waste

products, including Amyloid-β oligomers, through the so-called glymphatic system (Xie et al. 2013). Whether astrocyte Ca^{2+} signal is involved in these processes is a likely possibility that requires further studies. Recently, it has been revealed the prominent role of IP_3-dependent Ca^{2+} signaling in astrocytes for astrogliosis and neuronal survival after brain injury, showing impaired reactive astrogliosis and increased neuronal death in $IP_3R2^{-/-}$ mice (Kanemaru et al. 2013). Therefore, the dysregulation of astrocyte Ca^{2+} homeostasis and signaling may be associated with the AD pathology (Kuchibhotla et al. 2009; Lim et al. 2014). Several questions are still open and additional studies will be required to establish the role of IP$_3$R2-mediated astrocyte Ca^{2+} signaling in the onset and severity of AD.

In summary, present results indicate that basic features of neuron-astrocyte signaling, originally observed in young animals, are preserved in adulthood and during early stages of brain ageing. In contrast, dysfunction in gliotransmission and astrocyte-neuron communication is found in pathophysiological conditions, such as AD, highlighting the significance of astrocyte Ca^{2+} signaling for the proper brain activity, and suggesting that changes in homeostatic functions of astrocyte-neuron signaling might contribute to pathological progression of neurodegenerative diseases.

Acknowledgments

REFERENCES

Agulhon C, Fiacco TA, McCarthy KD. Hippocampal short- and long-term plasticity are not modulated by astrocyte Ca2+ signaling. Science. 2010; 327:1250–1254. [PubMed: 20203048]

Agulhon C, Petravicz J, McMullen AB, Sweger EJ, Minton SK, Taves SR, Casper KB, Fiacco TA, McCarthy KD. What is the role of astrocyte calcium in neurophysiology? Neuron. 2008; 59:932–946. [PubMed: 18817732]

Araque A, Carmignoto G, Haydon PG, Oliet SH, Robitaille R, Volterra A. Gliotransmitters travel in time and space. Neuron. 2014; 81:728–739. [PubMed: 24559669]

Bilkei-Gorzo A. Genetic mouse models of brain ageing and Alzheimer's disease. Pharmacol Ther. 2014; 142:244–257. [PubMed: 24362083]

Bosson A, Boisseau S, Buisson A, Savasta M, Albrieux M. Disruption of dopaminergic transmission remodels tripartite synapse morphology and astrocytic calcium activity within substantia nigra pars reticulata. Glia. 2015; 63:673–683. [PubMed: 25511180]

Braak H, Braak E. Neuropathological stageing of Alzheimer-related changes. Acta Neuropathol. 1991; 82:239–259. [PubMed: 1759558]

Bradley SJ, Challiss RA. G protein-coupled receptor signalling in astrocytes in health and disease: a focus on metabotropic glutamate receptors. Biochem Pharmacol. 2012; 84:249–259. [PubMed: 22531220]

Bussiere T, Bard F, Barbour R, Grajeda H, Guido T, Khan K, Schenk D, Games D, Seubert P, Buttini M. Morphological characterization of Thioflavin-S-positive amyloid plaques in transgenic Alzheimer mice and effect of passive Abeta immunotherapy on their clearance. Am J Pathol. 2004; 165:987–995. [PubMed: 15331422]

Chen N, Sugihara H, Sharma J, Perea G, Petravicz J, Le C, Sur M. Nucleus basalis-enabled stimulus-specific plasticity in the visual cortex is mediated by astrocytes. Proc Natl Acad Sci U S A. 2012; 109:E2832–E2841. [PubMed: 23012414]

Delekate A, Fuchtemeier M, Schumacher T, Ulbrich C, Foddis M, Petzold GC. Metabotropic P2Y1 receptor signalling mediates astrocytic hyperactivity in vivo in an Alzheimer's disease mouse model. Nat Commun. 2014; 5:5422. [PubMed: 25406732]

Di Castro MA, Chuquet J, Liaudet N, Bhaukaurally K, Santello M, Bouvier D, Tiret P, Volterra A. Local Ca2+ detection and modulation of synaptic release by astrocytes. Nat Neurosci. 2011; 14:1276–1284. [PubMed: 21909085]

Eroglu C, Barres BA. Regulation of synaptic connectivity by glia. Nature. 2010; 468:223–231. [PubMed: 21068831]

Fellin T, Pascual O, Gobbo S, Pozzan T, Haydon PG, Carmignoto G. Neuronal synchrony mediated by astrocytic glutamate through activation of extrasynaptic NMDA receptors. Neuron. 2004; 43:729–743. [PubMed: 15339653]

Gomez-Gonzalo M, Losi G, Chiavegato A, Zonta M, Cammarota M, Brondi M, Vetri F, Uva L, Pozzan T, de Curtis M. and others. An excitatory loop with astrocytes contributes to drive neurons to seizure threshold. PLoS Biol. 2010; 8:e1000352. [PubMed: 20405049]

Gomez-Gonzalo M, Navarrete M, Perea G, Covelo A, Martin-Fernandez M, Shigemoto R, Lujan R, Araque A. Endocannabinoids Induce Lateral Long-Term Potentiation of Transmitter Release by Stimulation of Gliotransmission. Cereb Cortex. 2015; 25:3699–3712. [PubMed: 25260706]

Grosche A, Grosche J, Tackenberg M, Scheller D, Gerstner G, Gumprecht A, Pannicke T, Hirrlinger PG, Wilhelmsson U, Huttmann K. and others. Versatile and simple approach to determine astrocyte territories in mouse neocortex and hippocampus. PLoS One. 2013; 8:e69143. [PubMed: 23935940]

Hung CW, Chen YC, Hsieh WL, Chiou SH, Kao CL. Ageing and neurodegenerative diseases. Ageing Res Rev. 2010; 9(Suppl 1):S36–S46. [PubMed: 20732460]

Jankowsky JL, Slunt HH, Ratovitski T, Jenkins NA, Copeland NG, Borchelt DR. Co-expression of multiple transgenes in mouse CNS: a comparison of strategies. Biomol Eng. 2001; 17:157–165. [PubMed: 11337275]

Jo S, Yarishkin O, Hwang YJ, Chun YE, Park M, Woo DH, Bae JY, Kim T, Lee J, Chun H. and others. GABA from reactive astrocytes impairs memory in mouse models of Alzheimer's disease. Nat Med. 2014; 20:886–896. [PubMed: 24973918]

Jurado-Parras MT, Delgado-Garcia JM, Sanchez-Campusano R, Gassmann M, Bettler B, Gruart A. Presynaptic GABAB Receptors Regulate Hippocampal Synapses during Associative Learning in Behaving Mice. PLoS One. 2016; 11:e0148800. [PubMed: 26848590]

Kanemaru K, Kubota J, Sekiya H, Hirose K, Okubo Y, Iino M. Calcium-dependent N-cadherin up-regulation mediates reactive astrogliosis and neuroprotection after brain injury. Proc Natl Acad Sci U S A. 2013; 110:11612–11617. [PubMed: 23798419]

Kozlov AS, Angulo MC, Audinat E, Charpak S. Target cell-specific modulation of neuronal activity by astrocytes. Proc Natl Acad Sci U S A. 2006; 103:10058–10063. [PubMed: 16782808]

Kuchibhotla KV, Lattarulo CR, Hyman BT, Bacskai BJ. Synchronous hyperactivity and intercellular calcium waves in astrocytes in Alzheimer mice. Science. 2009; 323:1211–1215. [PubMed: 19251629]

Li X, Zima AV, Sheikh F, Blatter LA, Chen J. Endothelin-1-induced arrhythmogenic Ca2+ signaling is abolished in atrial myocytes of inositol-1,4,5-trisphosphate(IP3)-receptor type 2-deficient mice. Circ Res. 2005; 96:1274–1281. [PubMed: 15933266]

Lim D, Ronco V, Grolla AA, Verkhratsky A, Genazzani AA. Glial calcium signalling in Alzheimer's disease. Rev Physiol Biochem Pharmacol. 2014; 167:45–65. [PubMed: 24935225]

Lopez-Ramos JC, Jurado-Parras MT, Sanfeliu C, Acuna-Castroviejo D, Delgado-Garcia JM. Learning capabilities and CA1-prefrontal synaptic plasticity in a mice model of accelerated senescence. Neurobiol Aging. 2012; 33:e13–e26.

Lynch AM, Murphy KJ, Deighan BF, O'Reilly JA, Gun'ko YK, Cowley TR, Gonzalez-Reyes RE, Lynch MA. The impact of glial activation in the aging brain. Aging Dis. 2010; 1:262–278. [PubMed: 22396865]

Maragakis NJ, Rothstein JD. Mechanisms of Disease: astrocytes in neurodegenerative disease. Nat Clin Pract Neurol. 2006; 2:679–689. [PubMed: 17117171]

Maynard S, Fang EF, Scheibye-Knudsen M, Croteau DL, Bohr VA. DNA Damage, DNA Repair, Aging, and Neurodegeneration. Cold Spring Harb Perspect Med. 2015:5.

Muneton-Gomez VC, Doncel-Perez E, Fernandez AP, Serrano J, Pozo-Rodrigalvarez A, Vellosillo-Huerta L, Taylor JS, Cardona-Gomez GP, Nieto-Sampedro M, Martinez-Murillo R. Neural differentiation of transplanted neural stem cells in a rat model of striatal lacunar infarction: light and electron microscopic observations. Front Cell Neurosci. 2012; 6:30. [PubMed: 22876219]

Navarrete M, Perea G, Fernandez de Sevilla D, Gomez-Gonzalo M, Nunez A, Martin ED, Araque A. Astrocytes mediate in vivo cholinergic-induced synaptic plasticity. PLoS Biol. 2012a; 10:e1001259. [PubMed: 22347811]

Navarrete M, Perea G, Maglio L, Pastor J, Garcia de Sola R, Araque A. Astrocyte Calcium Signal and Gliotransmission in Human Brain Tissue. Cereb Cortex. 2012b

Nett WJ, Oloff SH, McCarthy KD. Hippocampal astrocytes in situ exhibit calcium oscillations that occur independent of neuronal activity. J Neurophysiol. 2002; 87:528–537. [PubMed: 11784768]

Nimmerjahn A, Kirchhoff F, Kerr JN, Helmchen F. Sulforhodamine 101 as a specific marker of astroglia in the neocortex in vivo. Nat Methods. 2004; 1:31–37. [PubMed: 15782150]

Otsu Y, Couchman K, Lyons DG, Collot M, Agarwal A, Mallet JM, Pfrieger FW, Bergles DE, Charpak S. Calcium dynamics in astrocyte processes during neurovascular coupling. Nat Neurosci. 2015; 18:210–218. [PubMed: 25531572]

Palop JJ, Mucke L. Amyloid-beta-induced neuronal dysfunction in Alzheimer's disease: from synapses toward neural networks. Nat Neurosci. 2010; 13:812–818. [PubMed: 20581818]

Panatier A, Vallee J, Haber M, Murai KK, Lacaille JC, Robitaille R. Astrocytes are endogenous regulators of basal transmission at central synapses. Cell. 2011; 146:785–798. [PubMed: 21855979]

Pasti L, Volterra A, Pozzan T, Carmignoto G. Intracellular calcium oscillations in astrocytes: a highly plastic, bidirectional form of communication between neurons and astrocytes in situ. J Neurosci. 1997; 17:7817–7830. [PubMed: 9315902]

Paxinos, G., Franklin, K. Paxinos and Franklin's the Mouse Brain in Stereotaxic Coordinates. Elsevier B.V; 2012.

Perea G, Araque A. Properties of synaptically evoked astrocyte calcium signal reveal synaptic information processing by astrocytes. J Neurosci. 2005; 25:2192–2203. [PubMed: 15745945]

Perea G, Sur M, Araque A. Neuron-glia networks: integral gear of brain function. Front Cell Neurosci. 2014; 8:378. [PubMed: 25414643]

Perez-Alvarez A, Navarrete M, Covelo A, Martin ED, Araque A. Structural and functional plasticity of astrocyte processes and dendritic spine interactions. J Neurosci. 2014; 34:12738–12744. [PubMed: 25232111]

Peters O, Schipke CG, Philipps A, Haas B, Pannasch U, Wang LP, Benedetti B, Kingston AE, Kettenmann H. Astrocyte function is modified by Alzheimer's disease-like pathology in aged mice. J Alzheimers Dis. 2009; 18:177–189. [PubMed: 19584439]

Petravicz J, Fiacco TA, McCarthy KD. Loss of IP3 receptor-dependent Ca2+ increases in hippocampal astrocytes does not affect baseline CA1 pyramidal neuron synaptic activity. J Neurosci. 2008; 28:4967–4973. [PubMed: 18463250]

Pirttimaki TM, Codadu NK, Awni A, Pratik P, Nagel DA, Hill EJ, Dineley KT, Parri HR. alpha7 Nicotinic receptor-mediated astrocytic gliotransmitter release: Abeta effects in a preclinical Alzheimer's mouse model. PLoS One. 2013; 8:e81828. [PubMed: 24312364]

Riddle, D. Brain Aging: Models, Methods, and Mechanisms. Riddle, DR., editor. Boca Raton (FL): 2007.

Rudy CC, Hunsberger HC, Weitzner DS, Reed MN. The role of the tripartite glutamatergic synapse in the pathophysiology of Alzheimer's disease. Aging Dis. 2015; 6:131–148. [PubMed: 25821641]

Schaeffer EL, Figueiro M, Gattaz WF. Insights into Alzheimer disease pathogenesis from studies in transgenic animal models. Clinics (Sao Paulo). 2011; 66(Suppl 1):45–54. [PubMed: 21779722]

Shigetomi E, Bowser DN, Sofroniew MV, Khakh BS. Two forms of astrocyte calcium excitability have distinct effects on NMDA receptor-mediated slow inward currents in pyramidal neurons. J Neurosci. 2008; 28:6659–6663. [PubMed: 18579739]

Shigetomi E, Jackson-Weaver O, Huckstepp RT, O'Dell TJ, Khakh BS. TRPA1 channels are regulators of astrocyte basal calcium levels and long-term potentiation via constitutive D-serine release. J Neurosci. 2013; 33:10143–10153. [PubMed: 23761909]

Srinivasan R, Huang BS, Venugopal S, Johnston AD, Chai H, Zeng H, Golshani P, Khakh BS. Ca(2+) signaling in astrocytes from Ip3r2(−/−) mice in brain slices and during startle responses in vivo. Nat Neurosci. 2015; 18:708–717. [PubMed: 25894291]

Sun W, McConnell E, Pare JF, Xu Q, Chen M, Peng W, Lovatt D, Han X, Smith Y, Nedergaard M. Glutamate-dependent neuroglial calcium signaling differs between young and adult brain. Science. 2013; 339:197–200. [PubMed: 23307741]

Takano T, Han X, Deane R, Zlokovic B, Nedergaard M. Two-photon imaging of astrocytic Ca2+ signaling and the microvasculature in experimental mice models of Alzheimer's disease. Ann N Y Acad Sci. 2007; 1097:40–50. [PubMed: 17413008]

Takeda T. Senescence-accelerated mouse (SAM): a biogerontological resource in aging research. Neurobiol Aging. 1999; 20:105–110. [PubMed: 10537019]

Talantova M, Sanz-Blasco S, Zhang X, Xia P, Akhtar MW, Okamoto S, Dziewczapolski G, Nakamura T, Cao G, Pratt AE. and others. Abeta induces astrocytic glutamate release, extrasynaptic NMDA receptor activation, and synaptic loss. Proc Natl Acad Sci U S A. 2013; 110:E2518–E2527. [PubMed: 23776240]

Tang W, Szokol K, Jensen V, Enger R, Trivedi CA, Hvalby O, Helm PJ, Looger LL, Sprengel R, Nagelhus EA. Stimulation-evoked Ca2+ signals in astrocytic processes at hippocampal CA3-CA1 synapses of adult mice are modulated by glutamate and ATP. J Neurosci. 2015; 35:3016–3021. [PubMed: 25698739]

Ting JT, Daigle TL, Chen Q, Feng G. Acute brain slice methods for adult and aging animals: application of targeted patch clamp analysis and optogenetics. Methods Mol Biol. 2014; 1183:221–242. [PubMed: 25023312]

Tomobe K, Nomura Y. Neurochemistry, neuropathology, and heredity in SAMP8: a mouse model of senescence. Neurochem Res. 2009; 34:660–669. [PubMed: 19247832]

Tong X, Ao Y, Faas GC, Nwaobi SE, Xu J, Haustein MD, Anderson MA, Mody I, Olsen ML, Sofroniew MV. and others. Astrocyte Kir4.1 ion channel deficits contribute to neuronal dysfunction in Huntington's disease model mice. Nat Neurosci. 2014; 17:694–703. [PubMed: 24686787]

Verkhratsky A, Rodriguez JJ, Parpura V. Astroglia in neurological diseases. Future Neurol. 2013; 8:149–158. [PubMed: 23658503]

Xie L, Kang H, Xu Q, Chen MJ, Liao Y, Thiyagarajan M, O'Donnell J, Christensen DJ, Nicholson C, Iliff JJ. and others. Sleep drives metabolite clearance from the adult brain. Science. 2013; 342:373–377. [PubMed: 24136970]

Yates D. Neurodegenerative disease: Factoring in astrocytes. Nat Rev Neurosci. 2015; 16:67. [PubMed: 25601774]

Main Points

Fundamental Neuron-Astrocyte signaling pathway is largely conserved over the life span.

Dysfunction of astrocyte IP$_3$R2-dependent calcium signaling is associated with early progression of Alzheimer's disease.
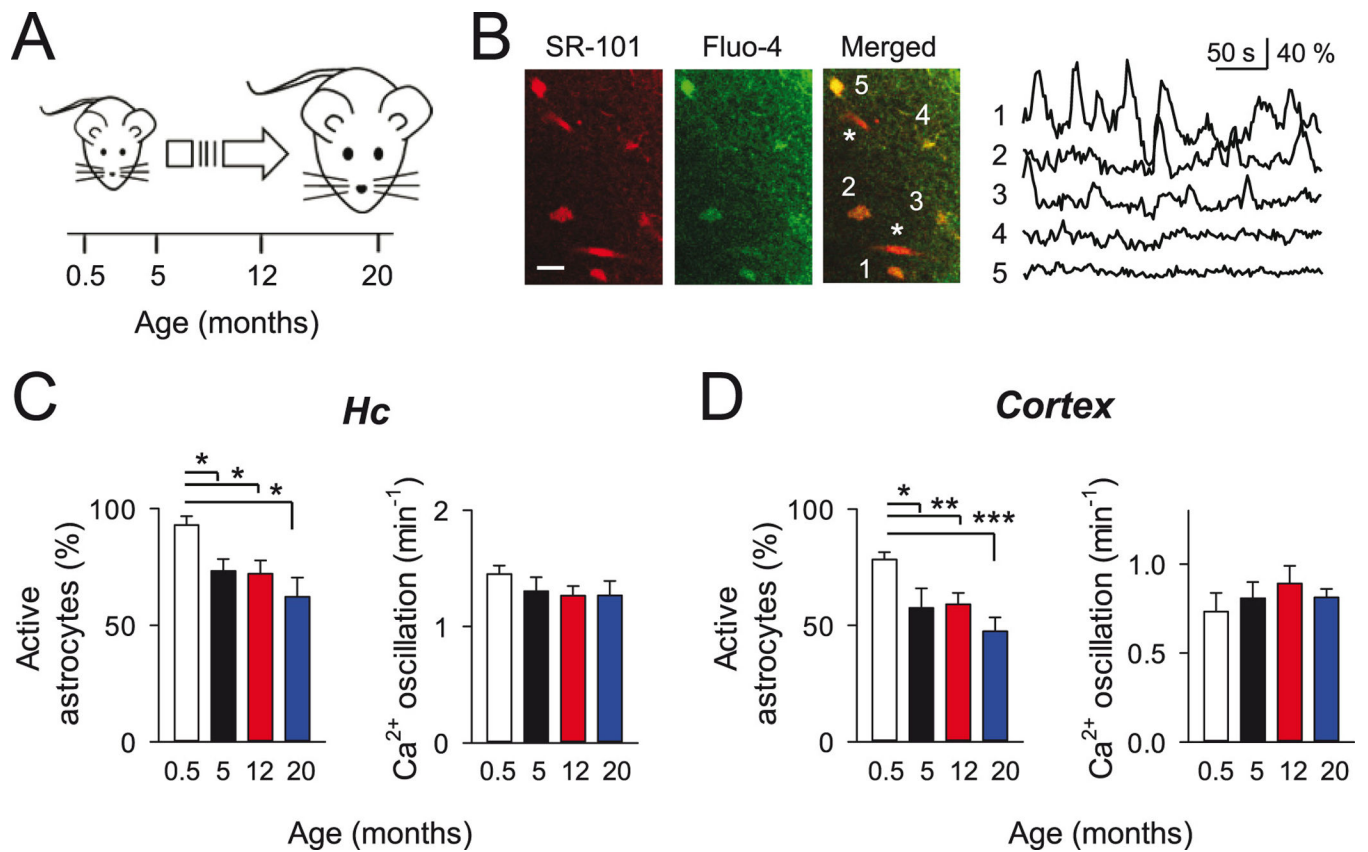
Figure 1. Spontaneous Ca²⁺ signals in astrocytes during aging

A: Scheme of different lifetime points selected for analysis. **B**: *Left*, pseudocolor images of hippocampal astrocytes (5-month old mouse) showing the colocalization of SR-101 and Fluo-4 fluoresecence signals at the soma of numbered astrocytes. Parenchymal blood vessels filled with SR101 are indicated (asterisk). Scale bar, 20 μm. *Right*, time course of the intracellular Ca²⁺ signals from astrocytes indicated in A. Note the presence of spontaneous Ca²⁺ oscillations in some astrocytes. **C–D**: Mean percentage of active astrocytes and Ca²⁺ oscillation frequency at different mice ages for hippocampus (C; n = 90, 86, 118 and 68 astrocytes from 0.5, 5, 12 and 20-month old mice, respectively), and cortex (D; n = 71, 60, 77 and 66 astrocytes from 0.5, 5, 12 and 20-month old mice, respectively). *p < 0.05; **p < 0.01; ***p < 0.001; unpaired t-test and Mann-Whitney rank-sum test. Error bars indicate SEM.
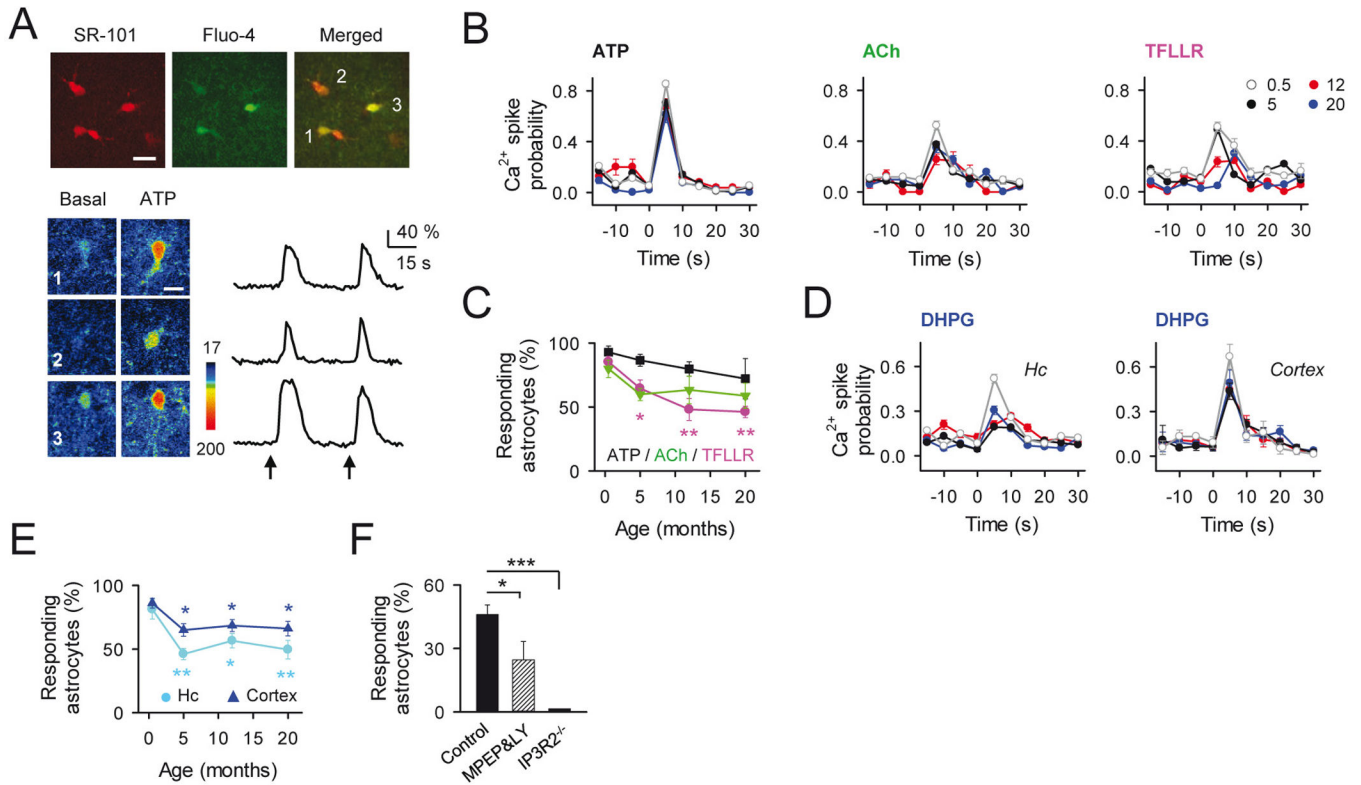
Figure 2. Neuron-Astrocyte Ca^{2+} signaling sensitivity during aging
A: *Top*, pseudocolor images of fluo-4- and SR-101-filled cortical astrocytes (5-month old mouse; scale bar, 15μm). *Bottom*, Ca^{2+} images and raw traces of labeled astrocytes before and after ATP stimulation (arrows; scale bar, 10 μm). **B**: Astrocyte Ca^{2+} spike probability to neurotransmitter receptor activation at different ages: ATP (4 mM; n 25 astrocytes) ACh (2 mM; n 16 astrocytes), and TFLLR (1 mM; n 35 astrocytes). **C**: Mean percentage of responsive astrocytes shown in B to the different agonist *vs* age. *p < 0.05; **p < 0.01; ANOVA followed by Student-Newman-Keuls test. **D**: Astrocyte Ca^{2+} spike probability to local application of DHPG (1 mM) during aging in hippocampus (n 53 astrocytes) and cortex (n 89 astrocytes). **E**: Mean percentage of responsive astrocytes shown in D to DHPG *vs* age. *p < 0.05; **p < 0.01; ***p < 0.001. ANOVA; followed by Student-Newman-Keuls test. **F**: Mean percentage of responsive astrocytes to DHPG in adult mice (5-month-old) in control conditions (n = 152; astrocytes; black bar), in MPEP (50 μM) + LY367385 (100 μM) (n = 79; astrocytes; dashed bar), and in IP$_3$R2$^{-/-}$ mice (n = 25; astrocytes; white bar). *p < 0.05; ***p < 0.001. ANOVA; followed by Student-Newman-Keuls test. Error bars indicate SEM.
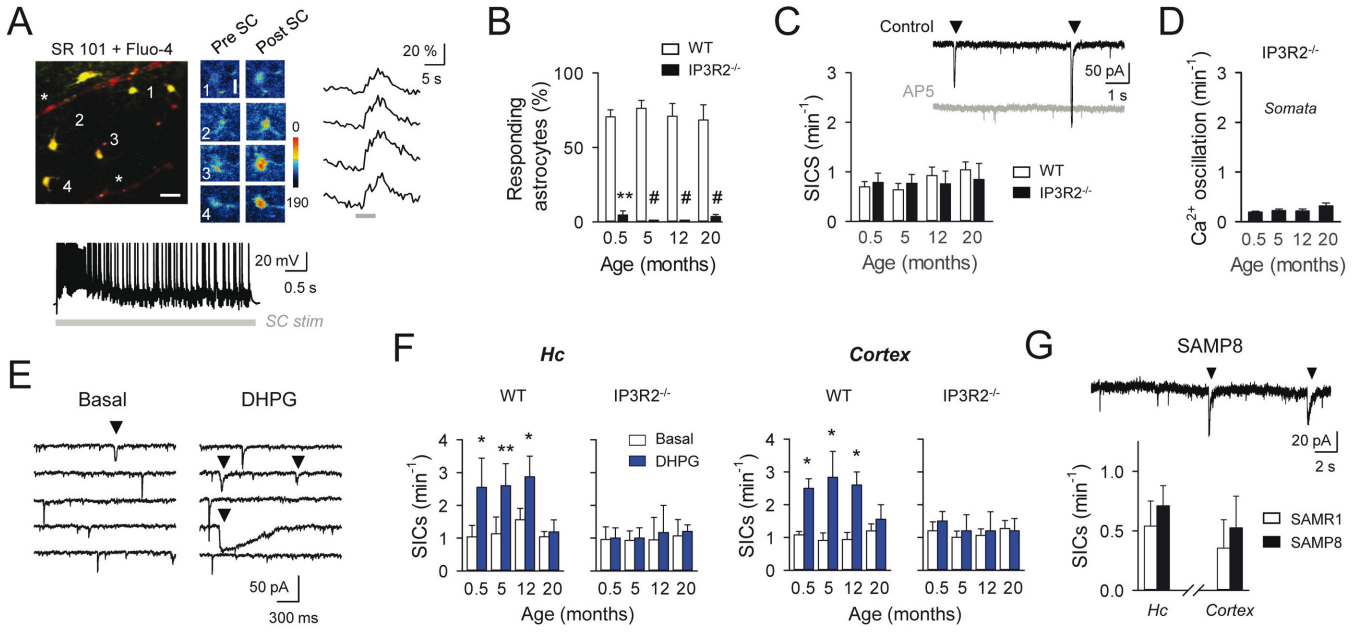
Figure 3. Astrocyte synaptic Ca^{2+} responses and gliotransmission during aging
A: *Top*, Pseudocolor images of fluo-4- and SR-101-filled hippocampal astrocytes (5-month old mouse. Scale bar, 25 μm), and Ca^{2+} images and raw traces of labeled astrocytes before and after Schaffer collateral (SC) stimulation (30 Hz, 5s; gray bar. Scale bar, 10 μm). Parenchymal blood vessels filled with SR101 are indicated (asterisk). *Bottom*, Whole-cell recordings from CA1 pyramidal cell showing neuronal activity induced during SC stimulation (30 Hz, 5 s; gray bar). **B**: Mean percentage of responding astrocytes to SC synaptic stimulation during aging, in wild type mice (white) and in IP$_3$R2$^{-/-}$ mice (black; n ≥ 32 and n ≥ 33 astrocytes for each condition in wild type and IP$_3$R2$^{-/-}$ mice, respectively). **p<0.01; #p < 0.001; Mann-Whitney rank-sum test. **C**: *Top*, Representative whole-cell recordings from CA1 hippocampal neurons from a 5 month-old mouse showing miniature excitatory currents (mEPSCs) and spontaneous SICs (down triangles), in control conditions and in the presence of the NMDAR antagonist AP5 (50 μM; gray trace). Note the absence of SICs in the presence of AP5. *Bottom*, Mean of SIC frequency at different ages in wild type mice (white; n ≥ 16 neurons for each condition) and in IP$_3$R2$^{-/-}$ mice (black; n ≥ 11). Note the absence of statistical differences; unpaired t-test. **D**: Mean astrocytic Ca^{2+} oscillation frequency from IP$_3$R2$^{-/-}$ mice at different ages (n = 23, 49, 64 and 70 astrocytes from 0.5, 5, 12 and 20-month old mice; respectively); p > 0.05; ANOVA followed by Student-Newman-Keuls test. **E**: Representative recordings from cortical neurons of SICs (down triangles), showing an increase in frequency after DHPG (1 mM) local stimulation. **F**: Mean frequency of hippocampal and cortical SICs in control and after DHPG stimulation (blue) in wild type mice (n ≥ 5 neurons for each condition) and in IP$_3$R2$^{-/-}$ mice (n ≥ 5) at different ages. *p < 0.05; **p < 0.01; paired t-test. **G**: Representative recordings from CA1 hippocampal neurons from a 6 month-old SAMP8 mouse showing spontaneous SICs (down triangles), and the SIC frequency average in SAMP8 mice (black; n = 6 neurons) and SAMR1 age-matched control mice (white; n = 7 neurons) in hippocampus and cortex. Note the absence of statistical differences; unpaired t-test. Error bars indicate SEM.
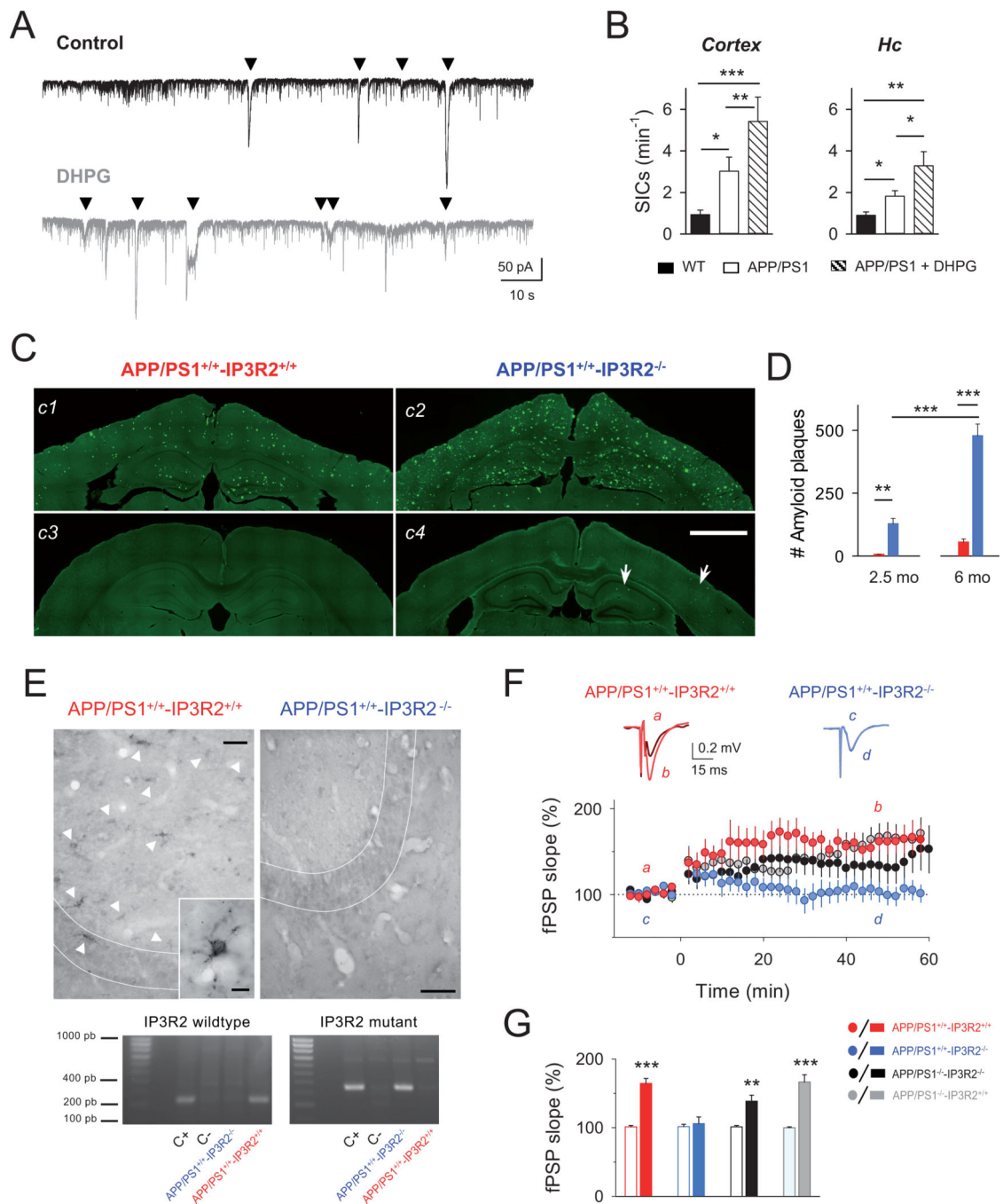
Figure 4. Astrocyte-neuron signaling dysfunction in APP/PS1 AD mouse model

A: Representative recordings from 12-month old APP/PS1 cortical neurons of SICs (down triangles) in control (black trace) and after local stimulation with DHPG (1 mM; gray trace). **B**: Average of cortical and hippocampal SIC frequency in control (white) and after DHPG stimulation in APP/PS1 mice (dashed; n   8 neurons for each condition), and compared with age-matched wild type mice (black; n   6). *p < 0.05; **p < 0.01; ***p < 0.001. ANOVA followed by Student-Newman-Keuls test. **C**: Representative fluorescence Thioflavin S staining images showing the Aβ deposits (green) in cortex and hippocampus of APP/PS1^{+/+}-

$IP_3R2^{+/+}$ and APP/PS1$^{+/+}$-$IP_3R2^{-/-}$ mice at 6-month old (c1, c2), and 2.5 month-old (c3, c4), respectively. Note the remarkable deposition of Thioflavin S-positive Aβ plaques in APP/PS1$^{+/+}$-$IP_3R2^{-/-}$ mice (c2 and c4; arrows). Scale bar, 1 mm. **D**: Mean values of plaque load in cortex and hippocampus in APP/PS1$^{+/+}$-$IP_3R2^{-/-}$ and APP/PS1$^{+/+}$-$IP_3R2^{+/+}$ mice (n = 8). **p < 0.01; ***p < 0.001; ANOVA followed by Bonferroni's test. **E**: *Top*, Protein detection of IP_3R2 in APP/PS1$^{+/+}$-$IP_3R2^{+/+}$ and APP/PS1$^{+/+}$-$IP_3R2^{-/-}$ mice by immunohistochemistry. Representative sections obtained from the same mice as shown in C, showing that APP/PS1$^{+/+}$-$IP_3R2^{+/+}$ mice exhibit immunoreaction product labeling astrocytes (white arrows) located in CA3 hippocampal region, while APP/PS1$^{+/+}$-$IP_3R2^{-/-}$ did not show immunoreactivity for IP_3R2 labeling. Scale bar, 100 μm. *Inset*, magnification picture showing a punctate pattern of IP_3R2 protein in astrocyte cell body and processes. Scale bar, 10 μm. *Bottom*, PCR amplification of the IP_3R2 wildtype gene and mutant allele from DNA obtained from brain sections shown in C. As expected, PCR confirms the specific ~200bp and ~400bp bands for $IP_3R2^{+/+}$ and $IP_3R2^{-/-}$ mice, respectively. C+,C- indicates positive and negative controls. **F**: *Top*, Representative fEPSP traces before (*a, c*) and after (*b,d*) high frequency stimulation (HFS) protocol in hippocampal slices from APP/PS1$^{+/+}$-$IP_3R2^{-/-}$ mice (blue), and APP/PS1$^{+/+}$-$IP_3R2^{+/+}$ (red) at 10 weeks. *Bottom*, Relative fEPSP slope (from basal values) versus time in APP/PS1$^{+/+}$-$IP_3R2^{-/-}$ mice (n = 12 slices from 4 mice; blue); APP/PS1$^{+/+}$-$IP_3R2^{+/+}$ mice (n = 9 slices from 3 mice; red); APP/PS1$^{-/-}$-$IP_3R2^{-/-}$ mice (n = 14 slices from 4 mice; black); APP/PS1$^{-/-}$-$IP_3R2^{+/+}$ mice (n = 12 slices from 4 mice; gray). Zero time corresponds to the onset of HFS. **G**: Relative changes of the fEPSP slope in APP/PS1$^{+/+}$-$IP_3R2^{-/-}$ mice and corresponding littermates shown in E. Error bars indicate SEM. ** p<0.01; ***p < 0.001; paired t-test.